Brief Communication

Soot Nucleation and Growth in Acetylene Air Laminar Coflowing Jet Diffusion Flames

K.-C. LIN, P. B. SUNDERLAND, and G. M. FAETH*
Department of Aerospace Engineering, The University of Michigan, Ann Arbor, MI 48109-2118

INTRODUCTION

The objective of the present investigation was to extend recent measurements of soot nucleation and growth within acetylene/air laminar jet diffusion flames [1]. Several factors motivated this extension. First, the measurements of Ref. 1 were limited to soot processes along the axes of laminar jet diffusion flames, where soot nucleates near the cool core of the flow and moves directly toward the flame sheet; therefore, it was of interest to consider other soot paths in order to investigate the generality of these results, especially for paths where soot nucleates near the flame sheet and initially moves toward more fuel-rich regions of the flow, which account for most of the soot production in buoyant diffusion flames [2]. In particular, nucleation near the cool core of the flame generally is accompanied by observations of translucent objects [1, 3, 4] but whether these objects are still observed for soot paths beginning at higher temperatures in the vicinity of the flame sheet must still be resolved. Secondly, measurements of hydrocarbons in Ref. 1 were limited to acetylene; therefore, information about the concentrations of other hydrocarbons is needed in order to establish their potential role in processes of soot formation within acetylene/air diffusion flames. Additionally, although several test flames were considered in Ref. 1, the available range of characteristic flame residence times (taken as the time for a fluid parcel to convect along the axis from the burner exit to the flame sheet) was rather narrow (17–23 ms); therefore, consideration of a broader range of flame conditions was of interest. Finally, a problem concerning measurements of O_2 concentrations at fuel-rich conditions was discovered, motivating reconsideration of effects of soot oxidation rates on measurements of soot growth rates.

EXPERIMENTAL METHODS

The experiments involved coflowing laminar jet diffusion flames burning at a pressure of 19 kPa within a windowed test chamber having a diameter and length of 300 and 1200 mm, respectively. The burner was directed vertically upward with acetylene flowing from a 6-mm-diameter port and air flowing from a concentric 60-mm-diameter port. The air passage contained several layers of beads and screens to provide a uniform velocity distribution at the burner exit while the flow through the fuel passage yielded fully developed laminar pipe flow at the burner exit. The entire burner assembly was traversed in the vertical and horizontal directions within the test chamber using stepping-motor driven linear positioners to accommodate rigidly-mounted instrumentation.

The following measurements were made for each test flame: soot volume fractions by laser extinction, soot structure by sampling and analysis using transmission electron microscopy (TEM), soot temperatures by multiline emission, gas compositions by sampling and gas chromatography, and streamwise and cross-stream gas velocities by laser velocimetry (LV). The determinations of soot volume fractions and temperatures involved deconvoluting line-of-sight measurements to obtain radial distributions of these properties.

The properties of the three test flames are summarized in Table 1. These flames involved a fixed acetylene flow rate with varying air coflow rates to provide air/fuel velocity ratios (at burner exit conditions), u_a/u_f, of 1.3, 3.4,

* Corresponding author.

COMBUSTION AND FLAME 104: 369–375 (1996)

Published by Elsevier Science Inc.

0010-2180/96/$15.00
SSDI 0010-2180(95)00225-1

TABLE 1

Summary of the Test Flames[a]

Test Flame	1	2	3
Air/fuel velocity ratio	1.3	3.4	6.3
Air flow rate (cm^3/s)	2100	5460	10100
Air velocity (mm/s)[b]	750	1950	3610
Luminous flame length (mm)	63	50	43
Stoich. flame length (mm)	77	66	53
Char. residence time (ms)	34	19	12

[a] Laminar coflowing jet diffusion flames with a 6 mm inside diameter fuel port, surrounded by a 60 mm inside diameter air port, operating at 19 kPa. Acetylene fuel flow rate of 3.85 cc/s with a fuel velocity of 575 mm/s and a fuel port Reynolds number of 93 (the last two parameters are based on a nominal temperature of 298 ± 2 K).

[b] Nominal average value based on an injector temperature of 298 ± 2 K.

and 6.3. Notably, the stoichiometric flame lengths (the length where a stoichiometric mixture is reached along the flame axis) were longer than the luminous flame lengths, highlighting the fact that significant soot oxidation proceeds at fuel-rich conditions in laminar diffusion flames. Characteristic flame residence times varied in the range 12–34 ms, achieving the desired increase in the residence time range from Ref. 1. Finally, tests with and without the acetylene purification train of Hamins et al. [5] showed that effects of acetone contamination of acetylene were not detectable for present test conditions.

RESULTS AND DISCUSSION

Soot and Flame Structure

The structure of the soot was similar to past observations in laminar diffusion flames [1, 3, 4]. In particular, the soot consisted of roughly spherical primary particles, having nearly constant diameters at a particular location within a test flame. These primary particles were collected into aggregates, with a broad distribution of the number of primary particles per aggregate, while the mean number of primary particles per aggregate increased with increasing residence time along a soot path.

Flame and soot structure were measured for two soot paths: (1) along the axis, where nucleation was initiated in the cool core of the flow, and (2) along the path through the maximum soot volume fraction condition, where nucleation was initiated near the flame sheet. The streamlines passing through the peak soot volume fraction locations were found from the two-dimensional LV measurements. Properties along both types of paths were qualitatively similar and are illustrated for the path along the axis of Flame 1 in Fig. 1. The following properties are illustrated as a function of the distance, z, from the burner exit: u, the streamwise velocity; d_p, the mean primary particle diameter; f_s, the soot volume fraction; n_p, the primary particle concentration; f, the mass fraction of fuel elements (or the mixture fraction); T, the temperature; and X_i, the mole fraction of species i. The residence time for fluid to convect from the burner exit to a particular value of z is shown along the top of the plot.

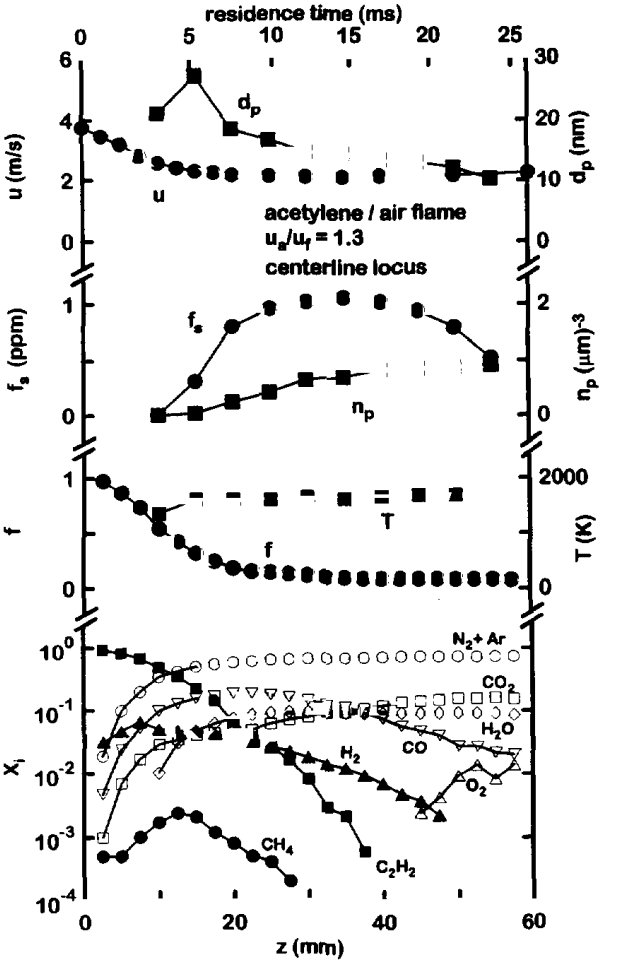

Fig. 1. Soot and flame properties along the axis of an acetylene/air laminar coflowing jet diffusion flame at 19 kPa and u_a/u_f of 1.3 (Flame 1).

The results illustrated in Fig. 1 are qualitatively similar to the observations of Ref. 1. Significant levels of soot formation begin when temperatures exceed roughly 1250 K (note that this temperature agrees quite well with the observations of Ref. 1 as well as the other test flames considered here) and end when the concentration of acetylene becomes small (at a fuel-equivalence ratio of roughly 1.14). Soot oxidation was rapid below a fuel-equivalence ratio of 1.14, so that all of the soot disappeared before the flame sheet was reached, see Table 1. The maximum value of d_p was reached before the end of the soot growth region because soot growth is less temperature-sensitive than soot nucleation; therefore, rapid nucleation toward the end of the soot formation region creates numerous primary particles whose relatively short lifetime yields small values of d_p even though the total mass of soot is increasing. Results for other soot paths, however, are different, e.g., the paths near the maximum f_s condition involve modest nucleation rates throughout the major growth period, so that both d_p and f_s tend to increase with increasing distance along the soot path.

Except for O_2, which will be discussed subsequently, present species concentration measurements are qualitatively similar to Ref. 1. In particular, the concentrations of major gas species—fuel (C_2H_2), N_2, CO_2, H_2O, CO, and H_2—are in good agreement with the generalized state relationships for hydrocarbon/air flames [6]. Furthermore, present measurements show that acetylene is the main hydrocarbon present in the soot formation region, with concentrations two to four orders of magnitude higher than methane, which was the only other hydrocarbon detected in significant concentrations. This behavior supports the dominant role played by acetylene in correlations of soot formation in acetylene/air diffusion flames [1].

Measurements of O_2 in Ref. 1, and possibly in several other sources used to generate the universal state relationships of Ref. 6, were found to be in error and were corrected during the present study. The difficulty was that Ar coelutes with O_2 for the gas chromatograph columns used in both Ref. 1 and the present study (Chromosorb 102 and molecular sieve 5A, HayeSep D, and molecular sieve 13X, respectively). A correction was made for this effect during the present study by assuming an Ar/N_2 molar ratio matching that of air and thus deducing the O_2 concentrations. This correction was most important in the soot formation region, reducing O_2 concentrations roughly an order of magnitude from the results reported in Ref. 1.

Soot Growth

Present measurements were used to study soot growth, similar to Ref. 1. The major assumptions of the growth rate analysis were as follows: soot surface growth rather than nucleation dominates soot mass production, which is reasonable because primary soot particles become visible when they are small; effects of thermophoresis and diffusion of soot are small so that soot convects along streamlines, which is reasonable because present flow velocities were large, on the order of 2 m/s, see Fig. 1; reaction surface area for soot growth was found assuming that primary particles were constant-diameter spheres that meet at a point, which is reasonable based on the observed properties of the soot aggregates; the local gas density was found from present concentration and temperature measurements, assuming an ideal gas mixture and neglecting the volume of soot; and soot density was taken to be 1850 kg/m^3. Temporal derivatives of soot and flow properties along soot paths were found from three-point least squares fits of the argument of the derivative. The resulting formulas used to find the gross soot growth rate, $w_g = \rho_s v_g$, where ρ_s is the soot density and v_g is the gross soot growth velocity, can be found in Ref. 1.

Based on past observations, soot growth was associated with acetylene concentrations [C_2H_2]; see earlier studies in diffusion flames [1] and in premixed flames [7–12]. In addition, acetylene had the highest concentrations of the hydrocarbons present in the soot growth region, and the end of soot growth coincided with the disappearance of acetylene for the present diffusion flames. Thus, w_g was correlated, as follows:

$$w_g = k_g(T)[C_2H_2]^n, \tag{1}$$

where $k_g(T)$ is an Arrhenius expression and n is the order of the reaction with respect to acetylene. No temperature dependence for k_g was found; therefore, a direct correlation of w_g as a function of $[C_2H_2]$ was sought, as illustrated in Fig. 2. In addition to present measurements, earlier results for acetylene/air diffusion flames [1] and for soot in premixed flames [7–12] are shown on the plot. Clearly, present results and those of Ref. 1 are in good agreement. This behavior shows that effects of soot path and residence time variations were not significant and that soot growth rates in acetylene/air diffusion flames were comparable to the growth rates of new soot in premixed flames (which are the highest of the premixed flame data points illustrated in Fig. 1, see Ref. 1 for a discussion of the relationship between the results for diffusion and premixed flames). Upon combining the present results and those of Ref. 1, the correlation illustrated in Fig. 1 can be found, as follows:

$$w_g = 1480[C_2H_2]^{1.52} \tag{2}$$

where w_g (kg/m^{2}s) and $[C_2H_2]$ (kg-mole/m^3). In Eq. 2, the 95% confidence interval for n is 1.26–1.78 and the correlation coefficient of the fit is 0.88. Thus, the order of the gross soot growth rate with respect to $[C_2H_2]$ was higher than past suggestions of a first-order acetylene reaction based on measurements of soot growth in premixed flames [7–12].

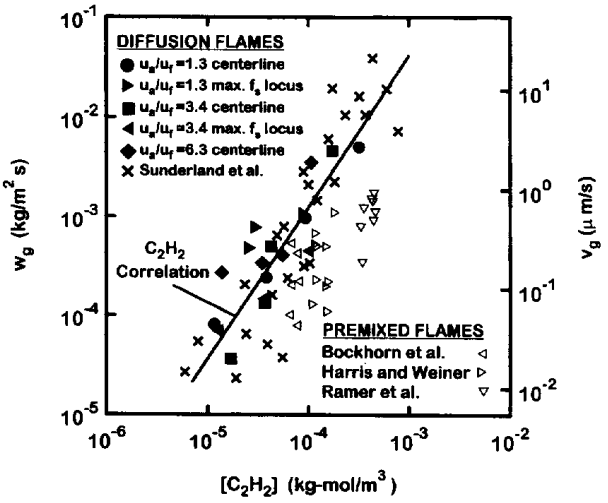

Fig. 2. Correlation of present gross soot growth rates in laminar acetylene/air diffusion flames, similar results for acetylene/air diffusion flames from Ref. 1, and similar results for premixed flames from Refs. 7–12.

The high order of gross soot growth with respect to acetylene concentrations can be attributed to effects of soot oxidation masking the true or net soot growth rate. Thus, corrections of the gross values of w_g for effects of soot oxidation were carried out following Ref. 1: soot oxidation by O_2 was estimated using the rate expression of Nagle and Strickland-Constable [13]; soot oxidation by CO_2 and H_2O was estimated following Johnstone et al. [14] and Libby and Blake [15, 16] which agreed with results based on Bradley et al. [17]. This procedure was checked by earlier measurements in the soot oxidation zone, finding that it generally overestimates soot oxidation rates by a significant margin [1]; therefore, results at conditions where the gross soot growth rate was negative were eliminated in order to minimize effects of uncertainties of soot oxidation rates.

Soot oxidation by OH was neglected when correcting the present growth rates, as justified by the following discussion. Recent measurements of Puri et al. [18] along the axes of buoyant hydrocarbon/air flames at atmospheric pressure indicated OH concentrations of approximately 3×10^{14} molecules/cm^3 at the point of peak soot volume fraction. The present soot formation regions involve lower H:C ratios and pressures than those of Ref. 18, and precede the point of peak soot volume fraction, all of which should yield OH concentrations below 3×10^{14} molecules/cm^3. Considering this concentration as an upper limit of present OH concentrations, and invoking an OH collision efficiency for soot oxidation of 0.13 from Neoh et al. [19], the growth rate obscured by OH oxidation in the present flames is at most 3×10^{-4} kg/m^{2}s. This rate is lower than most of the present gross soot rate data (see Fig. 2). Thus, the potential impact of soot oxidation by OH on the present net growth rates is small and its neglect does not significantly affect the conclusions which follow.

The present net soot growth rates are plotted as a function of acetylene concentration in Fig. 3. The coordinates of the plot anticipate a collision efficiency expression, as follows:

$$w_g = \eta C_{C_2H_2} \bar{v}_{C_2H_2} [C_2H_2]/4, \tag{3}$$

where η is the collision efficiency, $C_{C_2H_2}$ is the mass of carbon per mole of acetylene, and $\bar{v}_{C_2H_2}$ is the mean Boltzmann equilibrium molecular velocity of acetylene, which is found as follows:

$$\bar{v}_{C_2H_2} = \left(8kT/(\pi M_{C_2H_2})\right)^{1/2}, \quad (4)$$

where T is the gas temperature, k is Boltzmann's constant, and $M_{C_2H_2}$ is the molecular weight of acetylene. Other results shown on the plot include the earlier net soot growth rates for acetylene/air laminar jet diffusion flames from Ref. 1, and results from premixed flames from Refs. 7–12 where no correction has been made for soot oxidation.

Present measurements of net soot growth rates agree with those of Ref. 1 (see Fig. 3). Thus, the results of Ref. 1 are valid for various soot paths and a broader range of residence times. Finally, the growth rates in acetylene/air diffusion flames again did not exhibit an effect of age proposed from the observations within premixed flames [7–12].

Combining the present net soot growth rate measurements and those of Ref. 1 yields a best fit slope of the correlation with respect to $[C_2H_2]$ of 1.05 with a 95% confidence interval of 0.87–1.22 and a correlation coefficient of the fit of 0.88. Thus, the order of acetylene concentration in this correlation is not statistically different from unity and the following best first-order fit has been illustrated in Fig. 3:

$$w_g = 0.018\bar{v}_{C_2H_2}[C_2H_2], \quad (5)$$

where w_g (kg-mole/m^{2}s), $\bar{v}_{C_2H_2}$ (m/s) and $[C_2H_2]$ (kg-mol/m^3). In Eq. 5, the uncertainty of the coefficient (95% confidence) is 0.004 with a corresponding collision efficiency based on Eq. 4 of 0.0030 with an uncertainty (95% confidence) of 0.0006—all determined using geometric means. The corresponding collision efficiencies from Ref. 1 are not statistically different from the combined results found here.

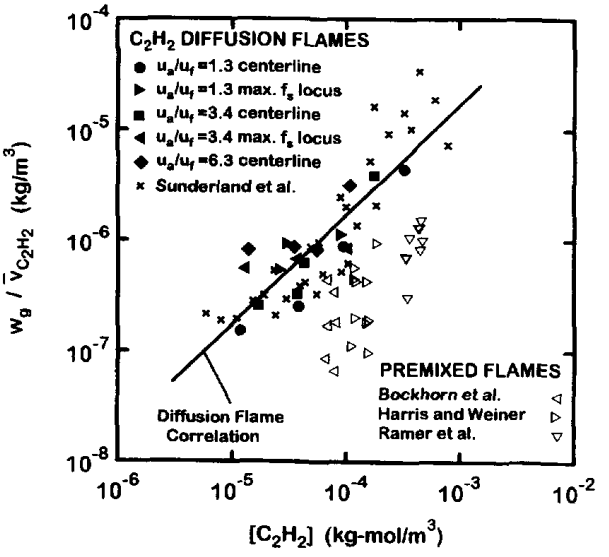

Fig. 3. Correlation of present net soot growth rates after correction for soot oxidation, in laminar acetylene/air diffusion flames, similar results for acetylene/air diffusion flames from Ref. 1, and soot growth rates for premixed flames from Refs. 7–12.

Soot Nucleation

Present measurements also were used to study soot nucleation rates, similar to Ref. 1. Notably, translucent objects were observed during the early stages of soot nucleation for all paths, although these objects were smaller for paths starting near the flame sheet than for paths starting near the cool core of the flame. The assumptions adopted to find soot nucleation rates were the same as for soot growth rates. The formulation is based on the rate of change of primary soot particle concentrations and does not explicitly consider effects of coagulation, reactions with heavy hydrocarbon species and PAH, etc., that may play a role in the formation of primary soot particles. The specific formulation used to reduce the data can be found in Ref. 1. Finally, soot nucleation generally was associated with the presence of acetylene and was best correlated as a first-order acetylene reaction; this involves using acetylene as a surrogate for PAH and other hydrocarbons that are actually involved in the formation of primary soot particles.

The correlation of soot nucleation rates, w_n, in terms of a first-order acetylene reaction, is plotted as a function of temperature in Fig. 4. In addition to the present results, the earlier measurements in acetylene/air diffusion flames of Ref. 1, and a correlation due to Leung et al. [20] based on optical measure-

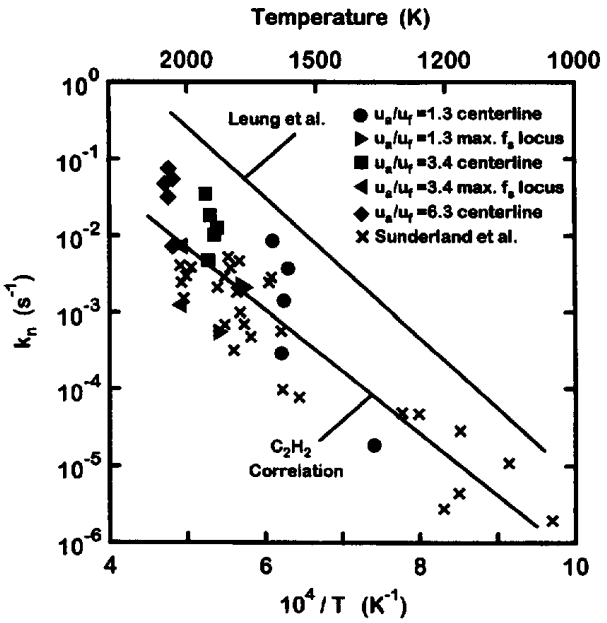

Fig. 4. Correlation of present soot nucleation rates within laminar acetylene/air diffusion flames, similar results for acetylene/air diffusion flames from Ref. 1, and earlier results for soot nucleation rates from Leung et al. [20].

ments from various sources, are shown on the plot. The two sets of measurements in the acetylene/air diffusion flames are in excellent agreement, yielding the combined soot nucleation correlation illustrated in Fig. 4, as follows:

$$w_n/[C_2H_2] = k_n = 73.6\exp(-18500/T) \quad (6)$$

where w_n (kg-mol/m^{3}s), $[C_2H_2]$ (kg-mol/m^3), k_n(s^{-1}), and T(K). In Eq. 6, the uncertainty (95% confidence) of the activation temperature is 2900 K. Notably, the activation temperature of Eq. 6, 18500 K, and the associated activation energy of 39 kcal/gmol, are not statistically different from corresponding values from Ref. 1. This finding implies that soot paths starting in the cool core of the flow, as well as at somewhat higher temperatures near the flame sheet, all involving translucent objects near the start of nucleation, have similar soot nucleation rate properties. Finally, the present nucleation rates in diffusion flames are significantly lower than the correlation of Leung et al. [20]; this discrepancy is attributed to approximations used to estimate the reactive soot surface area by Leung et al. [20] as discussed in Ref. 1.

CONCLUSIONS

Flame structure and soot processes were studied for various soot paths in acetylene/air laminar coflowing jet diffusion flames at 19 kPa, in order to supplement recent measurements limited to the axis of acetylene/air laminar jet diffusion flames [1]. The major conclusions of the study are as follows:

1. Considering all paths through the flames, significant levels of soot nucleation and growth require temperatures greater than roughly 1250 K and fuel-equivalence ratios greater than 1.14. Maximum primary soot particle diameters generally are observed before the end of the soot growth region, due to the greater temperature sensitivity of soot nucleation than soot growth, although this maximum is reached earliest for flow along the flame axis.
2. Present soot growth measurements, corrected for effects of soot oxidation, yielded first-order behavior with respect to acetylene in good agreement with Ref. 1, e.g., the collision efficiency for the combined data set was 0.0030 which is statistically identical to the value found in Ref. 1, both based on the geometric mean. Finally, measurements showed that concentrations of acetylene were two to four orders of magnitude larger than methane which was the next most abundant hydrocarbon observed, supporting the importance of acetylene for soot nucleation and growth processes within acetylene/air diffusion flames.
3. Soot nucleation was roughly first-order with respect to acetylene concentrations, in agreement with the observations of Ref. 1, e.g., the activation energy of the combined data set was 39 kcal/gmol, which is not statistically different from the value found in Ref. 1. Finally, the translucent objects found near the onset of formation for soot paths along the flame axis [1, 3, 4] also were observed for soot paths starting near the flame sheet and appear to be associated with early soot formation in diffusion flames.

This research was supported by Office of Naval Research Grant No. N00014-93-0321 under the

technical management of G. D. Roy, and NASA Grant No. NAG3-1245 under the technical management of D. L. Urban of the Lewis Research Center. The authors wish to thank a reviewer for pointing out the problem of coelution of O_2 and Ar for the gas chromatograph columns used here and in Ref. 1.

REFERENCES

1. Sunderland, P. B., Köylü, Ü. Ö., and Faeth, G. M., *Combust. Flame* 100:310–322 (1995).
2. Sunderland, P. B., Mortazavi, S., Faeth, G. M., and Urban, D. L., *Combust. Flame* 96:97–103 (1994).
3. Megaridis, C. M., and Dobbins, R. A., *Combust. Sci. Technol.* 66:1–16 (1989).
4. Dobbins, R. A., Fletcher, R. A., and Lu, W., *Combust. Flame* 100:301–309 (1995).
5. Hamins, A., Gordon, A. S., Saito, K., and Seshadri, K., *Combust. Sci. Technol.* 45:309–310 (1986).
6. Sivathanu, Y. R., and Faeth, G. M., *Combust. Flame* 82:211–230 (1990).
7. Bockhorn, H., Fetting, F., Wannemacher, G., and Wentz, H. W., *Nineteenth Symposium (International) on Combustion*, The Combustion Institute, Pittsburgh, 1982, pp. 1413–1420.
8. Bockhorn, H., Fetting, F., Heddrich, A., and Wannemacher, G., *Twentieth Symposium (International) on Combustion*, The Combustion Institute, Pittsburgh, 1984, pp. 979–988.
9. Harris, S. J., and Weiner, A. M., *Combust. Sci. Technol.* 31:155–167 (1983).
10. Harris, S. J., and Weiner, A. M., *Combust. Sci. Technol.* 32:267–275 (1983).
11. Harris, S. J., and Weiner, A. M., *Combust. Sci. Technol.* 38:75–87 (1984).
12. Ramer, E. R., Merklin, J. F., Sorensen, C. M., and Taylor, T. W., *Combust. Sci. Technol.* 48:241–255 (1986).
13. Nagle, J., and Strickland-Constable, R. F., *Proc. Fifth Carbon Conf.* 1:154–164 (1962).
14. Johnstone, J. F., Chen, C. Y., and Scott, D. S., *Ind. Engr. Chem.* 44:1564–1569 (1952).
15. Libby, P. A., and Blake, T. R., *Combust. Flame* 36:139–169 (1979).
16. Libby, P. A., and Blake, T. R., *Combust. Flame* 41:123–147 (1981).
17. Bradley, D., Dixon-Lewis, G., El-Din Habik, S., and Mushi, E. M. J., *Twentieth Symposium (International) on Combustion*, The Combustion Institute, Pittsburgh, 1984, pp. 931–940.
18. Puri, R., Santoro, R. J., and Smyth, K. C., *Combust. Flame* 97:125–144 (1994); also, Erratum, in press.
19. Neoh, K. G., Howard, J. B., and Sarofim, A. F., *Particulate Carbon* (D. C. Siegla and B. W. Smith, Ed.), Plenum, New York, 1980, pp. 261–277.
20. Leung, K. M., Lindstedt, R. P., and Jones, W. P., *Combust. Flame* 87:289–305 (1991).

Received 31 October 1994; revised 3 October 1995